UCLA
UCLA Electronic Theses and Dissertations

Title
Applications of Substrate Integrated Waveguide (SIW) Structure in Microwave Engineering

Permalink
https://escholarship.org/uc/item/71n2t4nb

Author
Shen, Zhi

Publication Date
2015

Peer reviewed|Thesis/dissertation

eScholarship.org Powered by the California Digital Library
University of California

UNIVERSITY OF CALIFORNIA

Los Angeles

Applications of Substrate Integrated Waveguide (SIW) Structure in Microwave Engineering

A thesis submitted in partial satisfaction

of the requirements for the degree Master of Science

in Electrical Engineering

by

Zhi Shen

2015

© Copyright by

Zhi Shen

2015

ABSTRACT OF THE THESIS

Applications of Substrate Integrated Waveguide (SIW)

Structure in Microwave Engineering

by

Zhi Shen

Master of Science in Electrical Engineering

University of California, Los Angeles, 2015

Professor Tatsuo Itoh, Chair

This thesis is focused on some applications of the Substrate Integrated Waveguide (SIW) structure in microwave engineering. It is mainly divided into two parts, covering a dual-band high Q filter and a broadband high gain ring slot antenna, both of which are based on SIW resonators. This work indicates strong potential of SIW structure in communication system and discusses its unique advantages in detail.

In the first part of the thesis, a dual-band high Q second order filter is designed to work at around 10 GHz and 14 GHz. SIW cavities are chosen in order to fulfill the low loss requirements. Two kinds of perturbation theories are applied in this structure to make two second order pass bands. Transmission lines of proper length are designed to connect the cavities together and make them work efficiently.

In the second part of the thesis, a broadband high gain SIW ring slot antenna working at around 18 GHz is discussed. The bandwidth of the antenna is approximately 12.7% and the gain is around 7 dB. The cavity mode is properly chosen to reach the high antenna gain requirement. The working mechanism of its broadband property is discussed in detail to reach a reasonable argument.

The thesis of Zhi Shen is approved.

Yahya Rahmat-Samii

Benjamin Williams

Tatsuo Itoh, Chair

University of California, Los Angeles

2015

CONTENTS

LIST OF FIGURES

LIST OF TABLES

ACKNOWLEDGMENTS

I would like to express my sincere gratitude to Prof. Tatsuo Itoh for all his support and guidance throughout my years here in UCLA. To Prof. Yahya Rahmat-Samii and Prof. Benjamin Williams for being my thesis committee and offering invaluable opinions. To my fellow lab mates for all their help, without which I can never finish these projects. Last but not least, I would like to thank my family and friends for all their support.

BACKGROUND

The rapid development of research on Substrate Integrated Waveguide (SIW) technology implies people's strong eagerness on implementation and integration of microwave and millimeter-wave components and wireless communication system. As we know, bulky metallic structure like waveguide and coaxial line are widely used for decades since they provide low loss and well-behaved electromagnetic properties. However, low-cost, small-size and highly-integrated circuit is more and more welcomed nowadays since it matches modern applications like mobile and wearable technology in a better way. Therefore, people are always looking for a balance between the advantages of these two kinds of structure.

SIW technique is a novel application to solve this problem. It can integrate planar structure like microstrip line and nonplanar structure like waveguide together, combining their advantages in return. Classical waveguide structure can now be implemented in planar form by using metalized vias or holes in dielectric substrates. It not only contains the advantages of classical microstrip circuit like low-cost, easiness of fabrication and compact-size, but also provides demanding waveguide properties that could only be achieved by bulky structure before[1-4]. It also allows integration of passive components like antenna and active components like amplifier on a single substrate, avoiding transitions between them and reducing losses and parasitic effects in return[1].

The first passive SIW component proposed in the literature was an inductive-post and iris filter, which allows higher quality factor compared with microstrip technology [2]. After that SIW technology started to attract people's attention, which led to its extensive application in every topic of microwave engineering. After detailed study, people have found out both conceptual and mathematical explanation for many of its invaluable properties.

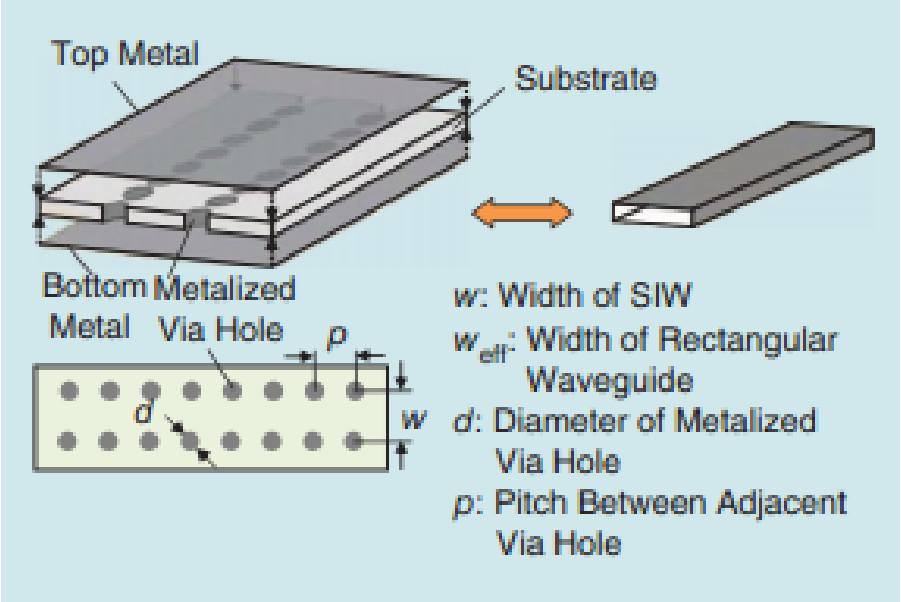

Fig. 1: Typical SIW structure [5].

A typical SIW structure is shown on the left of Fig. 1, which is equivalent to a classical waveguide shown on its right. There are two metal plates on the top and bottom of the substrate, and certain metalized via holes are used to connect them. This kind of structure is easy to fabricate through PCB technology. After long-term study, people have summarized the conditions under which the structure can function properly [5]:

$$\begin{aligned} p &> d \\ p/\lambda_c &< 0.25 \\ a_l/k_0 &< 1\times10^{-4} \\ p/\lambda_c &> 0.05, \end{aligned} \tag{1}$$

where a_l is the total loss and k_0 stands for the wave number in free space.

These conditions not only make the structure physically achievable, but also make the period fall into a reasonable range, making the ground metal vias act as a uniform metal boundary equivalently. Therefore, the overall structure performs just as a waveguide with metallic side walls around, and well-behaved waveguide modes are expected to exist [5].

However, since there may still be some leakage through the gap between adjacent vias, the equivalent size of the waveguide is reasonably large, which can be calculated through the following empirical formula:

$$w_{\text{eff}} = w - 1.08 \times \frac{d^2}{p} + 0.1 \times \frac{d^2}{w} \tag{2}$$

There are two important properties of SIW structure that we should pay attentions to. Firstly, since the actually truncated side walls cannot support longitudinal current, the SIW structure can only support traditional TM modes in the waveguide [5]. Moreover, since the thickness of the substrate is always much smaller than the width, only TM_{m0} modes are dominant for such a 2.5D structure. These two properties inherently prohibit SIW structure from some unwanted modes and make them have strong potential for many applications, which will be discussed in detail in the following sections.

The background above describes the properties of SIW structure in general. In the following chapters, two cases including a dual-band high Q filter and a broadband high gain antenna will be discussed in detail, which are used as examples to illustrate some possible applications of typical SIW based cavity structure.

CHAPTER ONE: SIW STRUCTURE IN FILTER DESIGN

Introduction

Filter designers always need to make tradeoffs between many factors such as selectivity, loss, cost, miniaturization, sensitivity to environmental effects, etc. In modern RF and microwave front end, a low-loss, low-cost filter with high channel selectivity is always needed in order to make full use of the invaluable spectrum. However, the inherent conflicts between some of the above-mentioned requirements make them difficult or even physically impossible to be satisfied at the same time [5]. For example, a high selectivity usually needs multiple resonators, which will raise the insertion loss in return. A high Q value is acquired with the help of larger volume and cost, which is in contrast to low-profile structure. Therefore, a novel designing methodology should be raised in order to make the best compromise.

Conventional filter design technology can be divided into two categories, namely, planar and nonplanar [5]. Nonplanar structures like waveguides are bulky and costly. They are usually chosen for high-performance and low-loss requirements. However, planar structure like transmission line is easier to fabricate and has lower cost, but its performance is always limited by the high loss and low efficiency. Then, the substrate integrated waveguide (SIW) structure was discovered, providing a best tradeoff between the loss and cost [6-9].

The well-studied SIW circuit fills right in the gap between planar and nonplanar type of technologies, combining the best of both and offering a brand-new technology for filter design. The unique advantages of it is obvious: the SIW structure only supports TM modes, making the parasitic responses from unwanted TE modes vanish outside the passbands (Here the direction perpendicular to the metal plates is defined as z direction. The word TM is used to represent TM^z.

It does not conflict with the arguments we made before). A thin substrate makes the modes to exist only as TM_{m0}, which are easy to control and calculate. The special 2.5D topology allows it to integrate with other planar circuits on the same substrate, increasing its flexibility in many electrical systems.

To make it more straightforward, a comparison between SIW structure and resonators that conventional filters are based on is shown in the following figure. We can easily find out that SIW resonator provides a possibility to make better compromise between the design requirements.

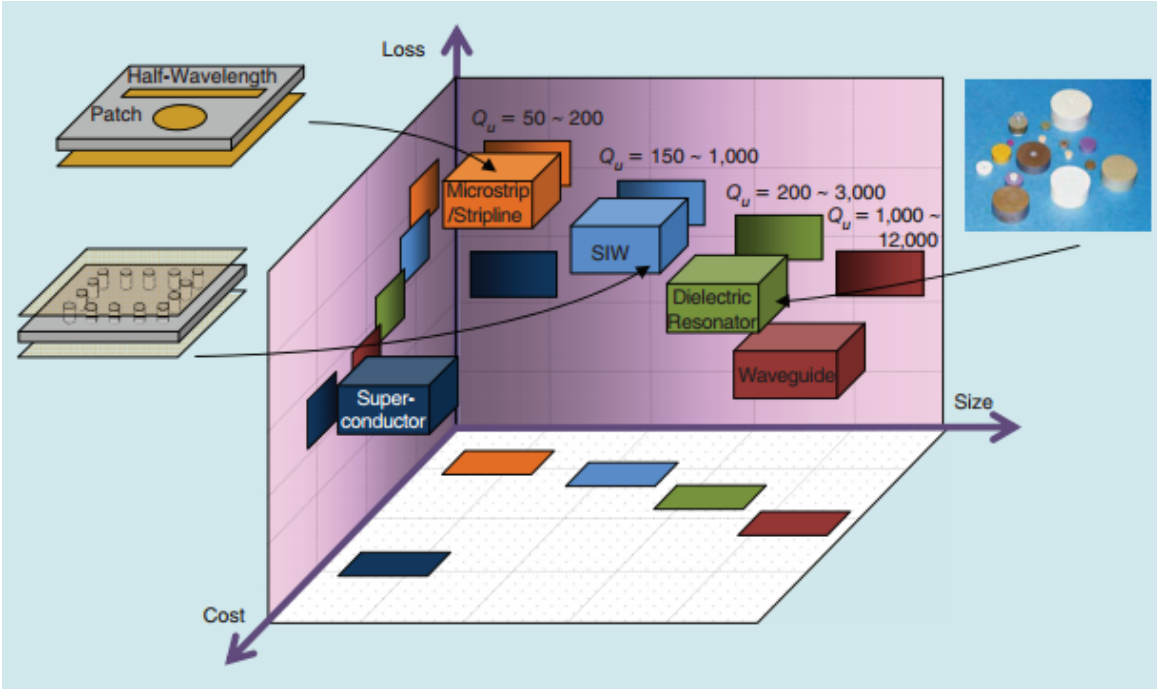

Fig. 2: The comparison between SIW structure and conventional resonators [5].

In order to have a better understanding of the applications of SIW structure in filter design, a dual-band high Q filter based on SIW resonator is studied. This design won the first prize in the student design competition hosted by the International Microwave Symposium (IMS) 2015 in Phoenix, Arizona. Detailed requirements and designing process are shown below.

Project Requirements & Design Challenges

This project aims at designing a packaged SIW dual band filter. Its specifications are listed below:

A) Passband 1 should have a fractional bandwidth of 4%, centered around 10 GHz;

B) Passband 2 should have a fractional bandwidth of 4%, centered around 14 GHz;

C) Both passbands are required to have at least a two-pole band-pass response;

D) The in-band insertion loss should be as low as possible;

E) The rejection between the two passbands are cared about, the higher the better.

The ideal response of the filter should be like what is shown in fig 3.

The filter was expected to be either a single-layer or a multi-layered printed circuit board (PCB) and housed in a pre-defined metallic package [10]. The measurements were made by a vector network analyzer through standard female SMA connectors connected to the package. The package was secured with a copper tape lid in good contact with the package body when the measurements were made.

The demand of 4% fractional bandwidth and low insertion loss for both passbands demands the use of high quality factor resonators for the implementation of the filter. Therefore, SIW structure is a good choice because of its well-behaved waveguide properties. However, the package that the circuit should be placed in is smaller than λ x λ in cross-section, where λ is the free space wavelength at the center frequency of lower band. This calls for techniques to miniaturize the size of the resonators. As for the rejection at frequencies between the two passbands, coupling between different resonators should be taken good care of.

Finally, a well-behaved dual band filter is designed, fabricated and measured to closely meet the desired specifications. Two kinds of perturbation theory are applied to create the dual modes

for the two passbands separately. Transmission lines of proper length are designed to make the cavities work independently. Careful fabrication and measurement make the measured results match simulation results very well, proving the reliability and universality of our designing methodology.

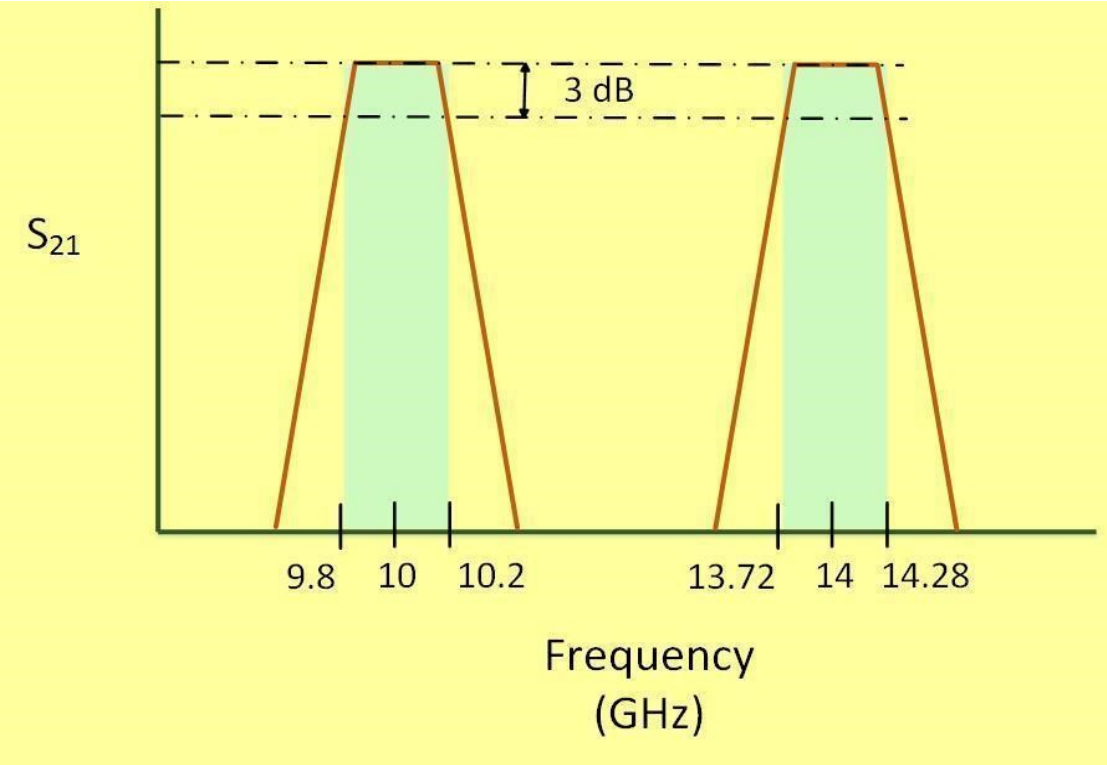

Fig. 3: Graphical representation of ideal filter characteristics according to competition specifications.

Dual-mode 14 GHz Cavity Resonator

The two most commonly used shapes of SIW cavity structures are rectangle and circle. The methods to create the second order frequency response are a little different.

In order to make a second order response, the basic idea is to create two modes working at frequencies very close to each other. To do so in rectangular cavity, the ratio between its edges should be very close to 1. On the other hand, when circular shape is used, dual mode response is formed by perturbing the degenerate modes of the cavity [11]. The common ways to add

perturbations are adding slots, cuts, or small patches that change the electric field pattern of the modes.

As we discussed above, only TM modes can be supported inside the SIW cavity, while TM_{mno} modes are the dominant. Therefore, when rectangular cavity is used, there is no way to create a band-pass response as narrow as 4% since the modes cannot be that close. Therefore, circular cavity is a better choice for these requirements.

As we know, the circular cavity has the axial field distribution of the form:

$$A_m(\varphi) = \sin(m\,\varphi) + \cos(m\,\varphi) \tag{3}$$

where *A* represents a field associated with the *m*th mode of the resonator. φ denotes the angle in the axial direction. From equation 3, it is clear to see that the odd (sin) and even (cos) modes can be independently controlled by proper perturbations, since they are orthogonal to each other. If we add perturbation at the symmetric plane, where even modes become maximum and odd modes become zero, the frequencies for even modes will change while those for odd modes will be kept unchanged. On the contrary, when asymmetric plane is perturbed, opposite results would happen. Therefore, by adding perturbation on a small scale at the proper place, narrow band response like 4% can be achieved.

To get a dual mode response, since TM010 mode does not provide the flexibility to tune even and odd modes independently, TM110 mode is chosen. In order to avoid spurious in the pass bands, the ratio between these modes should be adjusted carefully. From calculation, TM110 and TM010 mode appear to be at around 14 GHz and 8.79 GHz respectively [12]. Since we only care about the in-band response and rejection between the frequencies, TM010 mode will not create any problem to the filter response.

For the filter design, a 25-mil-thick Rogers TMM 10 [13] with a relative dielectric constant of 9.8 and loss tangent of 0.0022 substrate material is used. High dielectric constant is chosen to minimize the size. Thick substrate leads to wider transmission line, which means smaller amount of loss and convenience in fabrication. The final design of the cavity with dimensions is shown in Fig 4.

As we can see, the vias near the asymmetric plane are moved inside for a certain distance, making the equivalent size for the odd mode a little smaller, and increasing its working frequency in return. On the other hand, the even mode will not be influenced too much. Therefore, a small amount of frequency difference is created. The radius of the circular cavity and the distances of the vias are carefully designed in order to make the even mode of TM110 to work at a frequency 2% lower than 14GHz (13.72 GHz), and the odd mode of it to work at 2% higher (14.28 GHz). The bandwidth can be controlled by moving the perturbing vias [14]. The field distributions of these two modes are also shown below in Fig 5, offering much more straightforward explanation about their orthogonality and working mechanism.

The working mechanism of the designed filter is also shown in Fig. 6. Since the two modes are orthogonal to each other, there is no direct coupling between them. The signs of the coupling towards source and load control the number and location of the transmission zeroes, depending on the length and width of the insets that we designed [14]. A coupling scheme like this is finally chosen, since the transmission zeros can be located on both sides of the pass band, sharpening its roll off as well as increasing the out-of-band rejection.

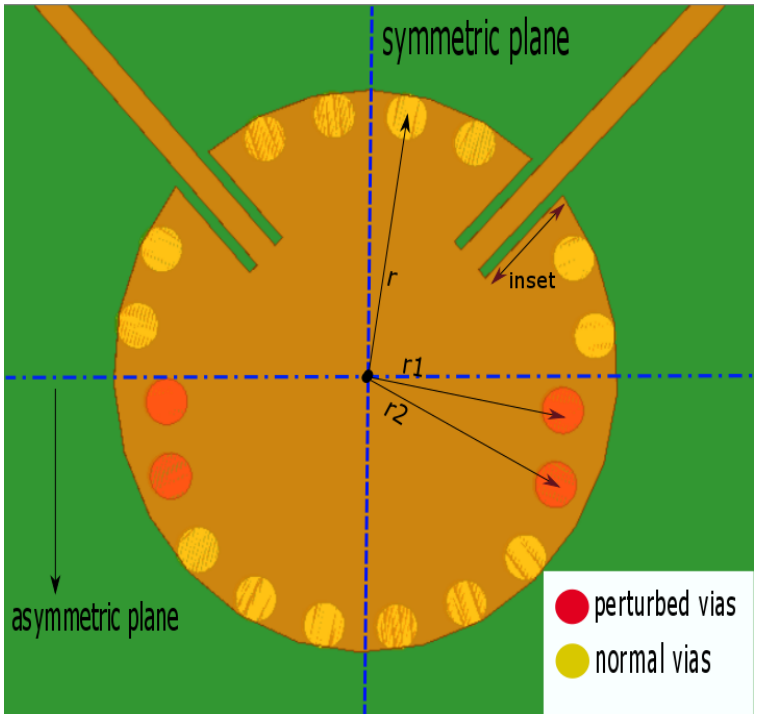

Fig. 4: Schematic of the SIW cavity for 14 GHz, r=4.5mm, r1=4.1mm, r2=4.3mm, inset=2.1mm.

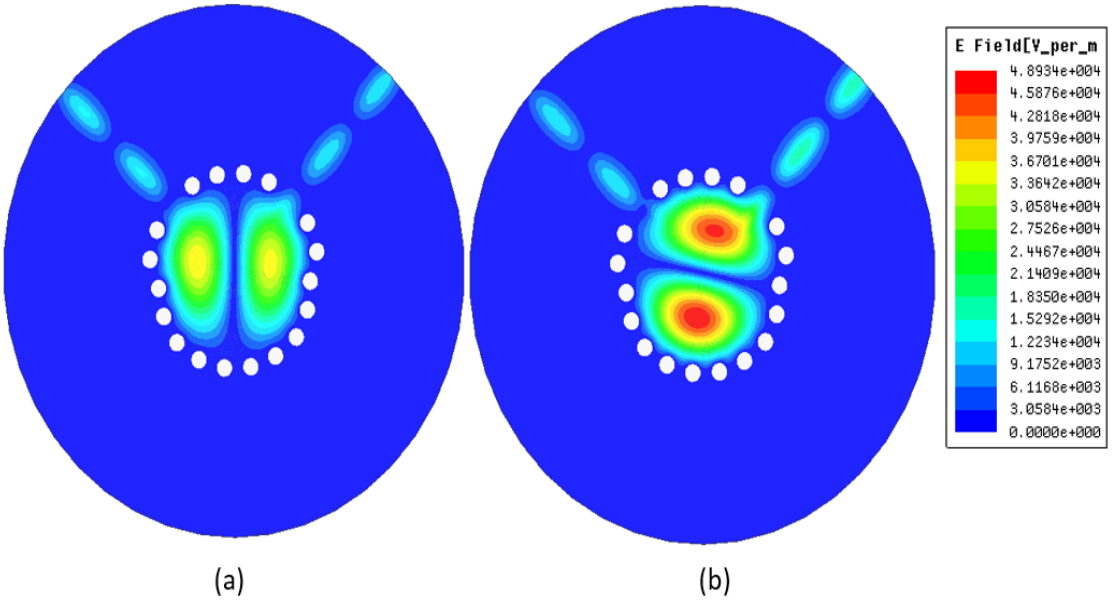

Fig. 5: Electric field distribution for (a) the odd mode (14.28GHz) and (b) the even mode (13.72GHz).

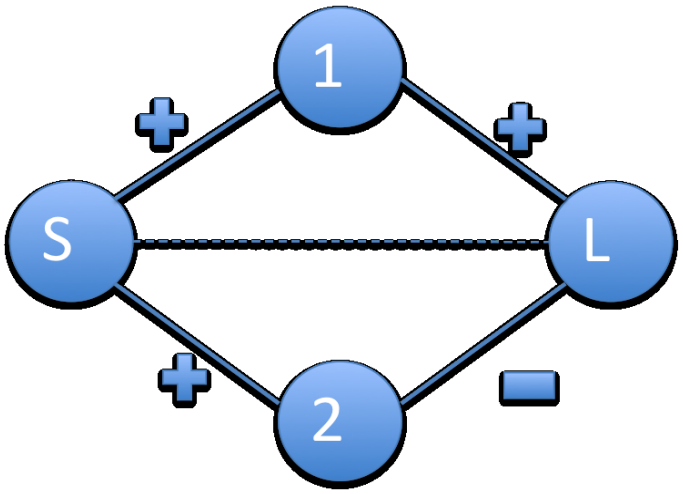

Fig. 6: Coupling scheme for the filter centered on 14GHz. Resonator 1 stands for the even mode while the resonator 2 stands for the odd mode. The dashed line represents the small source/load coupling

Simulation results of this single cavity are shown in Fig. 7. The center frequency of the passband is 14.02 GHz, while the 3-dB fractional bandwidth is 4.0%. The insertion loss is around 1.61 dB. Also, the out-of-band rejection between 10 GHz and 13.5 GHz (the frequency band we are interested in) is more than 25 dB with the presence of a transmission zero.

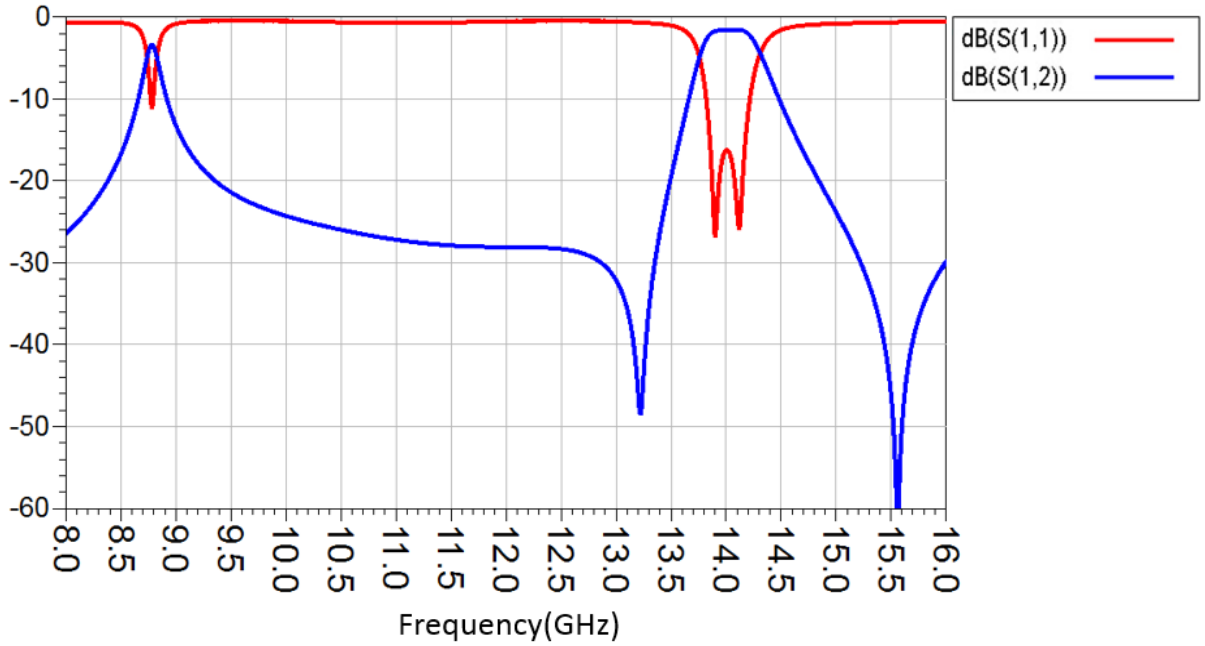

Fig. 7: Simulated return loss and insertion loss of the 14 GHz SIW cavity.

Dual-mode 10 GHz Cavity Resonator

Employing the same perturbation theory mentioned in the previous section, a dual-mode resonator at 10 GHz can also be designed. The only difference will be that the dimensions need to be scaled up. However, the higher order modes are something we should care about. If we still make TM110 mode resonant at 10 GHz as what we have done before, its higher order mode, TM210, will be located at around 13.5GHz [12], which is very close to the other pass band that we are interested in. However, we want two cavities to work independently without having any resonance at the frequencies in between. Since the TM210 mode here will definitely destroy the overall performance, another method is proposed to create the second order resonator at around 10 GHz.

A perturbation method of using ground metal pins inside the cavity is presented here. As we know from the previous section, only TM modes can exist inside the SIW cavity, which means there will be electric fields perpendicular to the cavity surface. That is, if we place metal pins vertically as Fig 8, the electric fields will be tangential along the vias. However, according to the boundary conditions, the tangential electric field on the metal surface has to be zero. Therefore, the field pattern inside the cavity will be distorted, creating a frequency shift for the corresponding cavity modes.

The key of this method is to find the correct locations for the ground pins. As we discussed before, the problem is with the frequency ratio of TM110 and TM210 mode. When we make use of TM110 mode, TM210 will cause unwanted resonance in the band we are interested in. Therefore, we can try to increase the frequency of TM210 mode while keeping TM110 unchanged. According to the filed distribution shown in Fig 9, the symmetric plane is the best choice since only TM110 mode has zero electric field there. Hence, when we put vias, TM110

will not get affected, but the TM210 will shift to higher frequency because of the smaller equivalent size of the cavity.

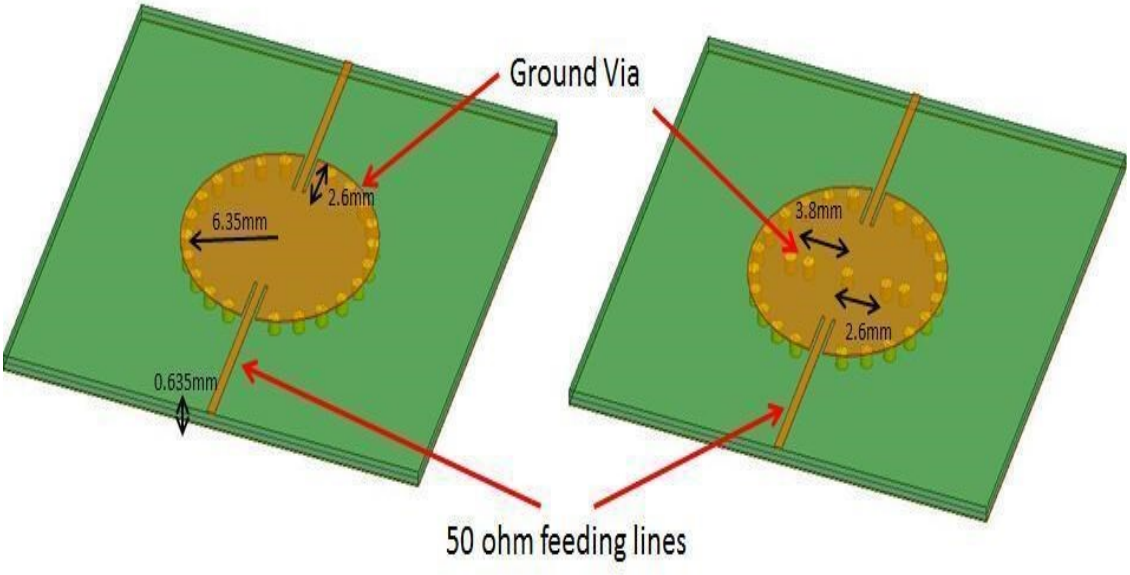

(a) (b)

Fig. 8: Schematics of the SIW cavity for 10 GHz (a) without and (b) with the perturbing copper vias.

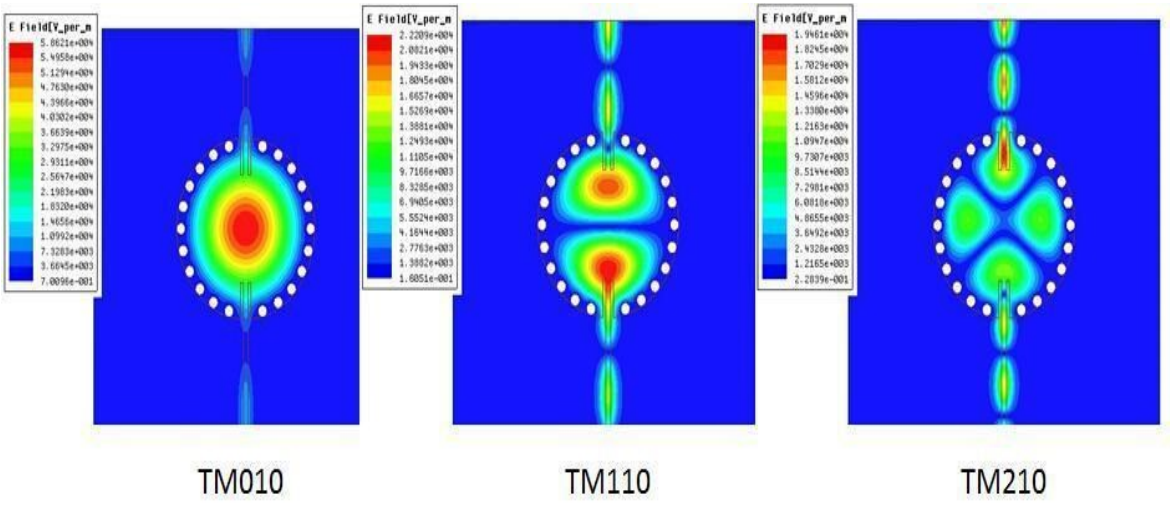

Fig. 9: The field distribution of TM010 mode, TM110 mode and TM210 mode for the 10 GHz cavity.

We also notice that for TM010 mode, the resonant frequency shifts to the higher side resulting from the reason we discussed above. Therefore, we can just make the perturbation large enough and combine TM010 and TM110 mode together to create a second order response. So finally we design the topology of the cavity as shown in Fig 8 (b), and the response of which is shown in Fig. 10. This clearly supports our argument. To summarize, before putting in the perturbation, TM010, TM110 and TM210 mode were at around 6.5GHz, 10GHz and 13.5GHz, respectively. After adding the ground vias, TM110 and TM010 form a second order resonance at around 10 GHz, while increasing TM210 to around 17 GHz, leaving the frequency band below it clean with no spurious resonance.

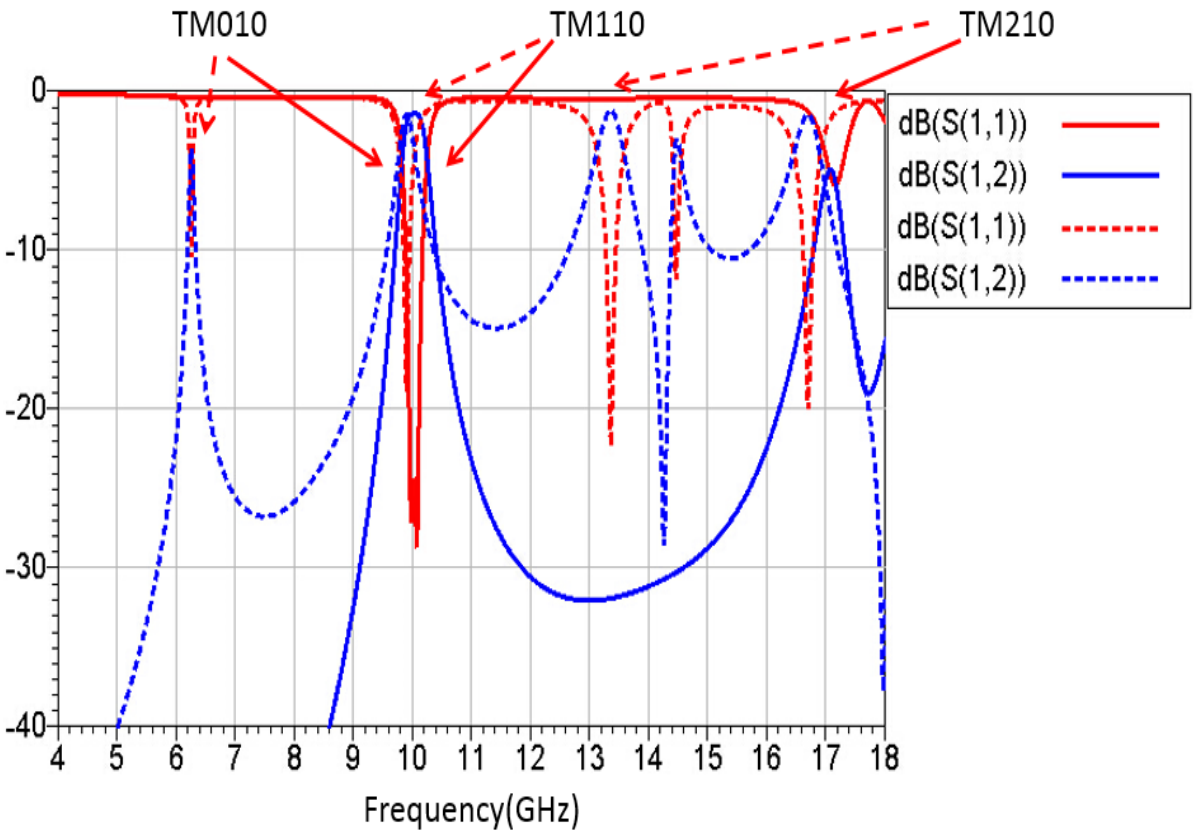

Fig. 10: The S parameters of the cavity with (solid line) and without (dash line) the perturbing vias.

Dual-band Filter

Once the two cavity resonators are designed separately, they need to be put together and form a dual-band filter. This is accomplished by extending the 50Ω microstrip feed lines for both cavities to meet at T-junctions, which is shown in Fig 11. By controlling the length of the feed line of each cavity, one branch can appear as open at the T-junction for the other band's operating frequency, making the two cavities work independently.

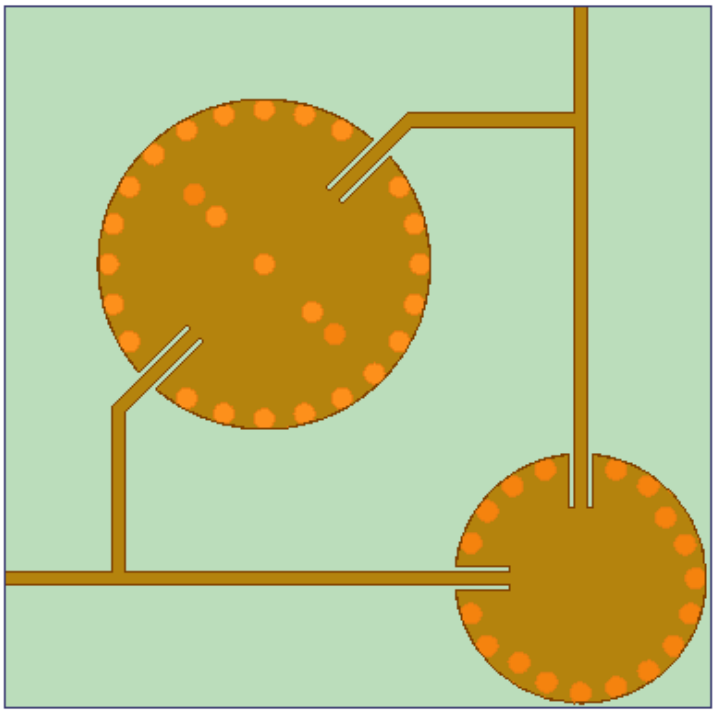

Fig 11: Schematic of the dual-band filter with the extended microstrip lines.

Fig. 12 can give a more straightforward explanation for how the dual-band filter works at the two different passbands.

Finally, the simulated S-parameter response for the dual-band filter is shown in Fig. 13. Some of the useful parameters are:

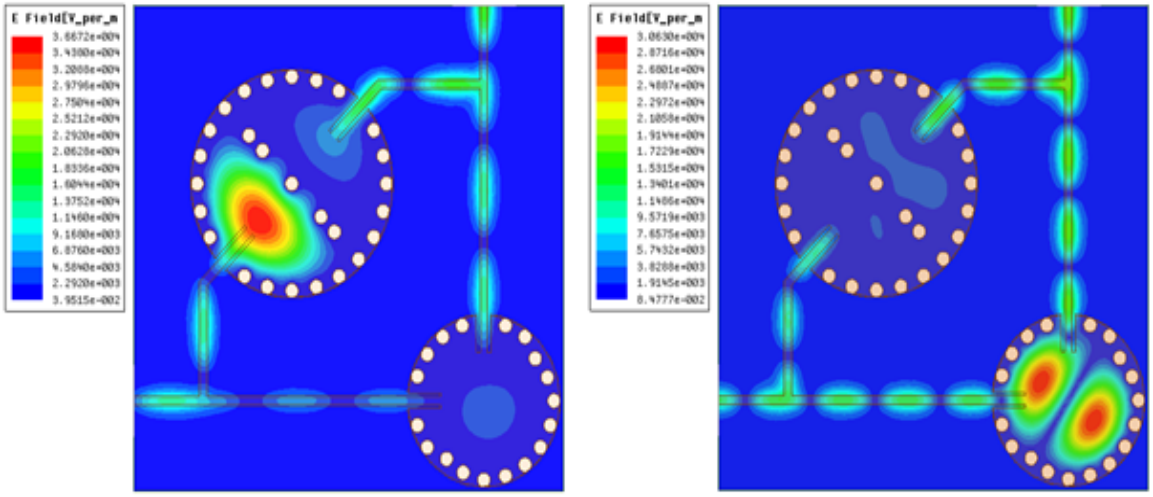

(a) (b)

Fig 12: Field distribution for the dual-band filter at 10 GHz (a) and 14 GHz (b).

a) Central frequency of the two passbands: 10.02 GHz and 14.02 GHz respectively;

b) Fractional bandwidths of the two bands: 4.1% for both bands;

c) In-band insertion loss for the two bands: 1.8 dB (10 GHz) and 1.9 dB (14 GHz);

d) Rejection of the frequencies in between the two bands: around 50 dB.

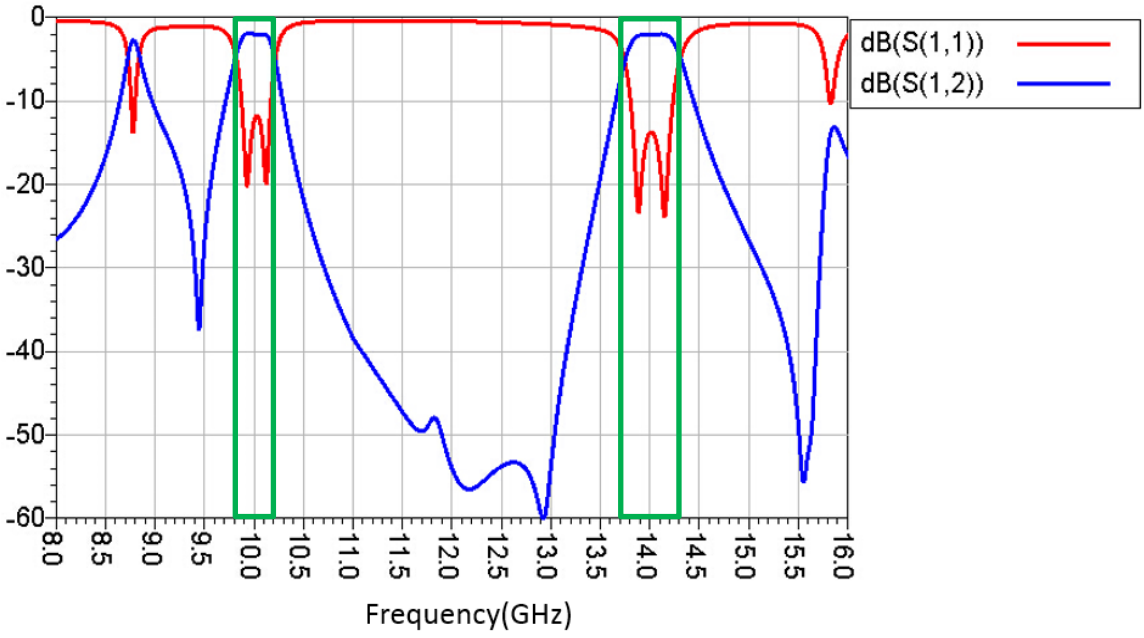

Fig 13: Simulated return loss and insertion loss of the second-order dual-band filter.

Measurement

The designed filter was first fabricated without the package to validate its performance. Then it was inserted into the demanded package. Finally copper cover is added on top of it. The prototypes are shown as Fig 14.

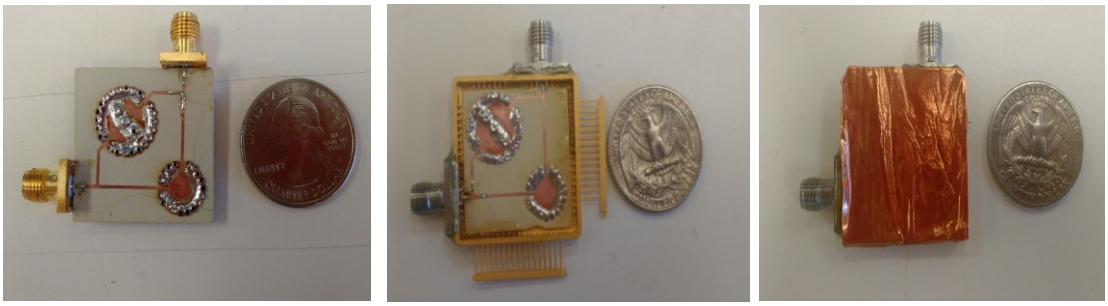

(a) *(b)* *(c)*

Fig. 14: (a) unpackaged and (b) packaged filters without and (c) with the copper cover. Their sizes are compared with that of the U.S. quarter coin.

Fig. 15 shows the comparison between the unpackaged case and simulation results. The center frequencies shifted slightly lower than simulated to 9.92 and 13.9 GHz for the two passbands. This happened because of the irregular dielectric constant of the substrate over the frequencies. The fractional bandwidths measured to be 3.9% for 10 GHz pass band and 5.7% for 14 GHz pass band. The increased bandwidth at 14 GHz could be because of the higher losses originating from the poor contact. This also explains the higher in-band insertion loss, which is 2.6 dB for the 10 GHz band and 3.7 dB for 14 GHz band. The rejection between the two passbands is over 24 dB.

Although the overall performance of the dual-band filter is not as good as that in the simulations, it shows very similar response. Fig. 15 shows the comparison between measured

and simulated results. Moreover, with a better fabrication process, especially for the vias, better performance can be achieved.

The measured result of the filter with package is shown in Fig. 16, which doesn't show significant difference. Finally, all the simulated and measured results are summarized in Table 1 for the reference.

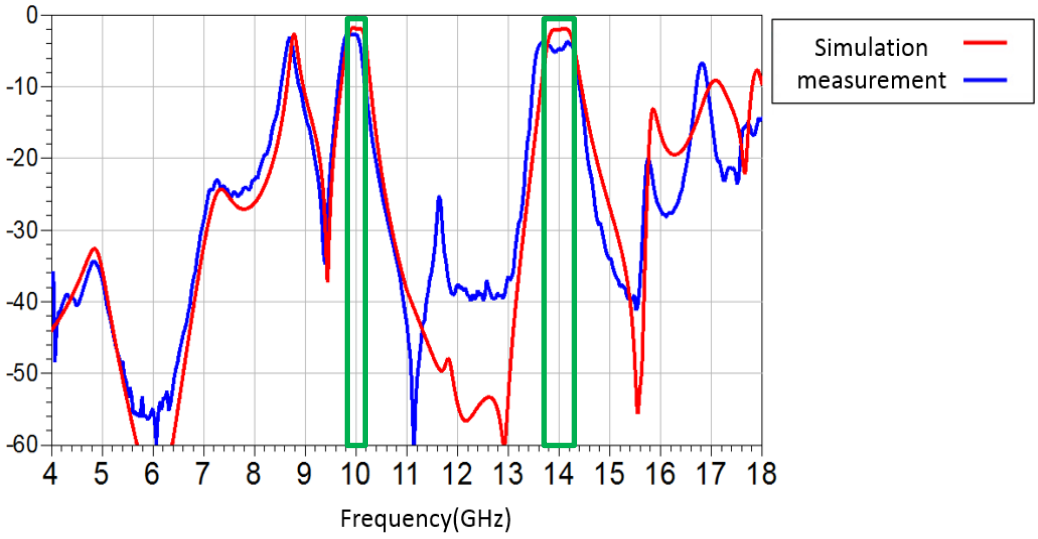

Fig. 15: Comparison between simulated and measured insertion loss of the unpackaged filter.

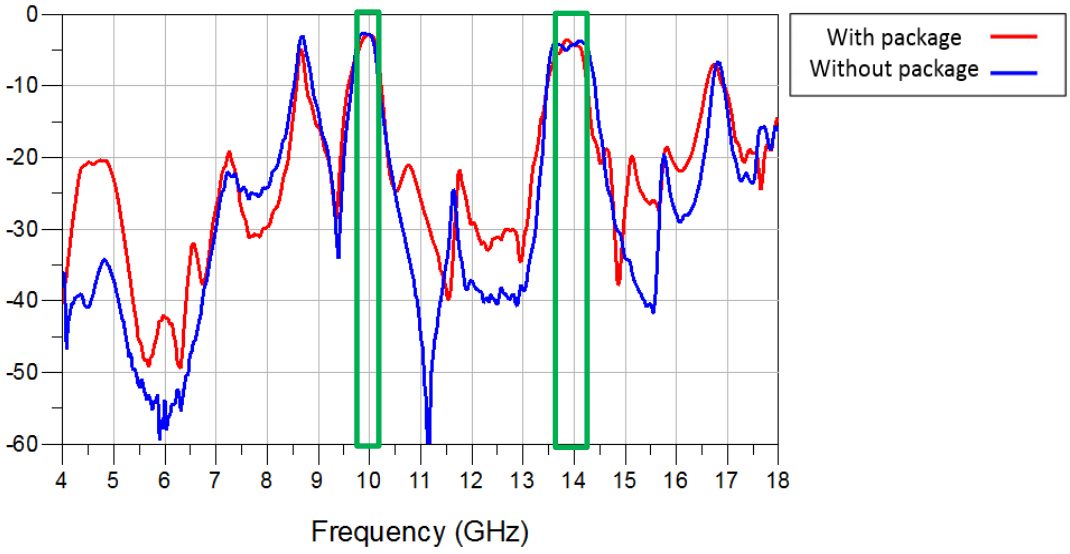

Fig. 16: Measured insertion loss of the unpackaged and the packaged filter.

Table 1: Summary of the performance of the SIW dual-band filter.

	Band 1			Band 2			
	Freq (GHz)	BW	IL (dB)	Freq (GHz)	BW	IL(dB)	Rejection (dB)
Simulation	10.0	4.1%	1.80	14.0	4.1%	1.92	>40
Measurement without package	9.92	3.9%	2.64	13.9	5.7%	3.70	>24
Measurement with package	9.94	4.3%	2.89	13.9	4.2%	3.53	>21

Conclusion

Two types of dual-mode SIW cavity resonators were designed and implemented to provide the desired second order band pass response at 10 GHz and 14 GHz respectively. Both cavities are of circular shape. Two types of perturbation methodologies based on inside metal vias are employed to form the dual modes. Microstrip-line-based feed section is carefully designed to make the cavities work independently at different passbands. The filter is then fabricated to meet the size requirements. The simulated and measured results of the filter match quite well.

CHAPTER TWO: SIW STRUCTURE IN ANTENNA DESIGN

Introduction

The SIW structure provides valuable waveguide and cavity properties through planar manufacturing process, which makes it very popular in antenna design [15]. Various types of SIW backed antennas are proposed in recent years. We are going to discuss a specific case, the ring slot antenna, in the following sections.

We will first discuss about the typical SIW backed slot antenna and its working mechanism. Considering its bandwidth limitation, a ring slot broadband antenna is then proposed and analyzed in detail. The working mode inside the cavity is properly chosen to offer the antenna high gain and patch-like pattern, which is desirable in communication systems. The broadband property is then discussed with a reasonable explanation.

Typical SIW Slot Antenna

A representative SIW slot antenna is shown in Fig. 17. Typically the length of the slot is quarter wavelength, and the width is very small. The slot is located at the center of the cavity and orthogonal to the feeding line, in order to create a monopole-like radiation pattern. Its return loss is shown in Fig. 18, which shows very narrow bandwidth.

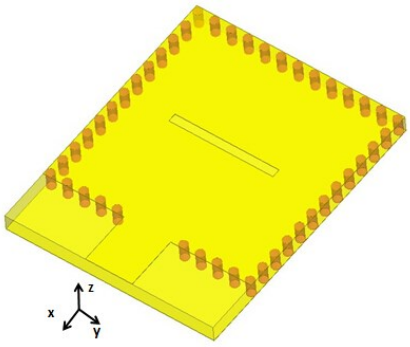

Fig. 17: The typical straight slot antenna topology.

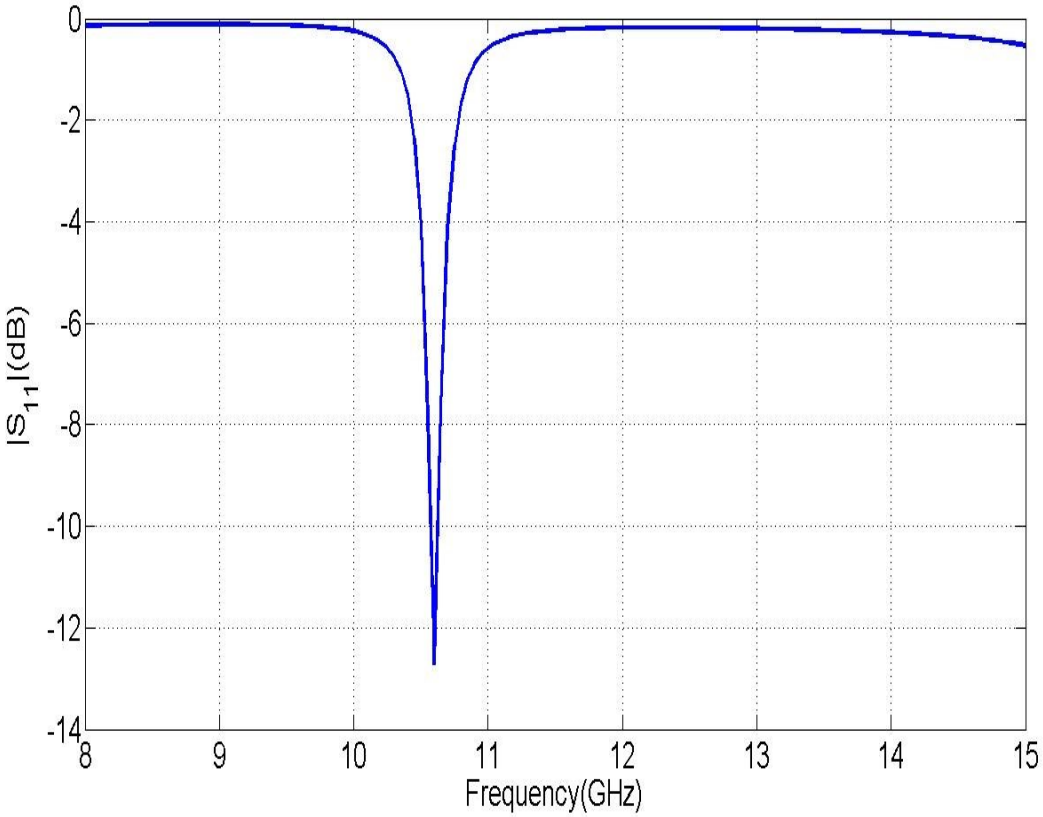

Fig. 18: S parameter for the straight slot antenna.

The antenna radiation property can be understood through the cavity mode analysis. Let us focus on the first two cavity modes: TM110 and TM210 (The directions of the coordinates are shown in Fig. 17. TM stands for TM^z here). Through waveguide mode analysis, we know that the field distribution of these modes should be similar to what is shown in Fig. 19. For TM110 mode, the electric field has a half-sinusoid distribution, while TM210 is sinusoidal in shape. The location of the slot is marked in the figure.

For TM110 mode, the slot is located right at the peak of the field, which means the field gradient is equal to 0. For TM210 mode, the slot is located at the place with highest field gradient, which is the zero-crossing point. Since the field gradient will create longitudinal

equivalent magnetic current on the slot aperture, a larger electric field gradient would lead to more efficient radiation. Therefore, the TM210 mode is desired in antenna design.

However, from the return loss of TE210 mode (Fig. 18) we can see that the bandwidth is quite narrow. Such structure typically provides 1~2% fractional bandwidth [16]. Although, broader bandwidth can be achieved by increasing the slot width [17], it is still limited. Bandwidth of such antenna does not only depend on the working mode, but also rely on the slot length. Therefore, broadband characteristics can be achieved by changing slot length to some extent.

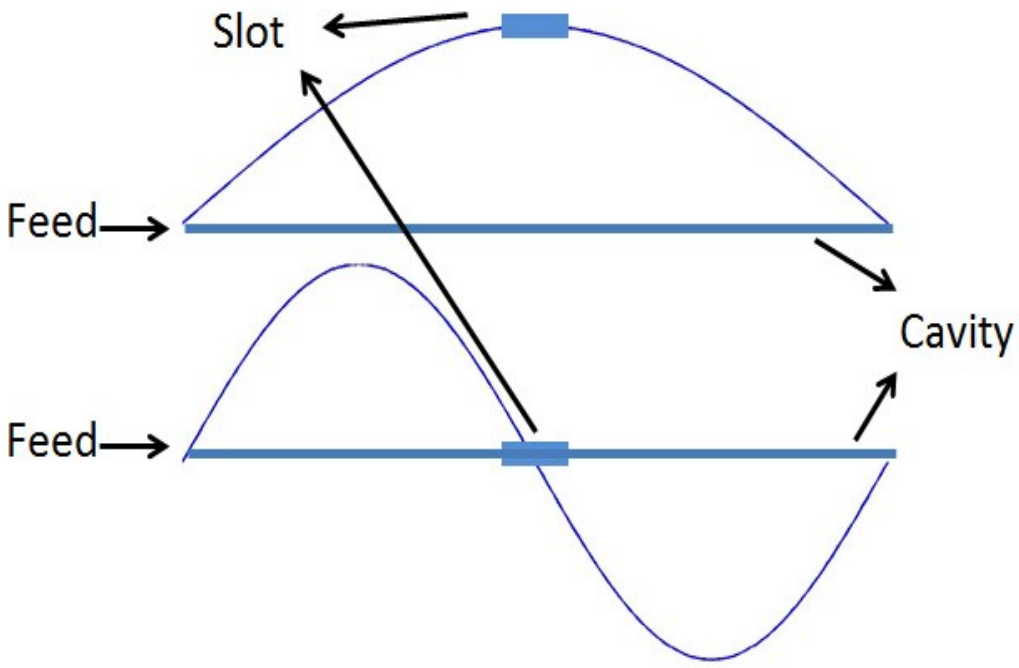

Fig. 19: The SIW straight slot antenna working modes. Top: The TM110 mode and the slot position in the mode. Bottom: The TM210 mode and the slot position in the mode.

Broadband SIW Ring Slot Antenna Topology and Performance

An SIW cavity backed ring slot antenna is designed to meet the broadband property. Its topology is shown in Fig. 20. The vertical vias connect the top and bottom conductors, forming an equivalent electrical wall. Typical cavity modes can be excited inside such SIW structure. The dimensions of the antenna are as shown in the figure. The cavity is of a square shape. A 50-ohm transmission line is used as the feed. Inset Feed is applied in order to match the impedance. A circular slot is placed right at the top center of the cavity.

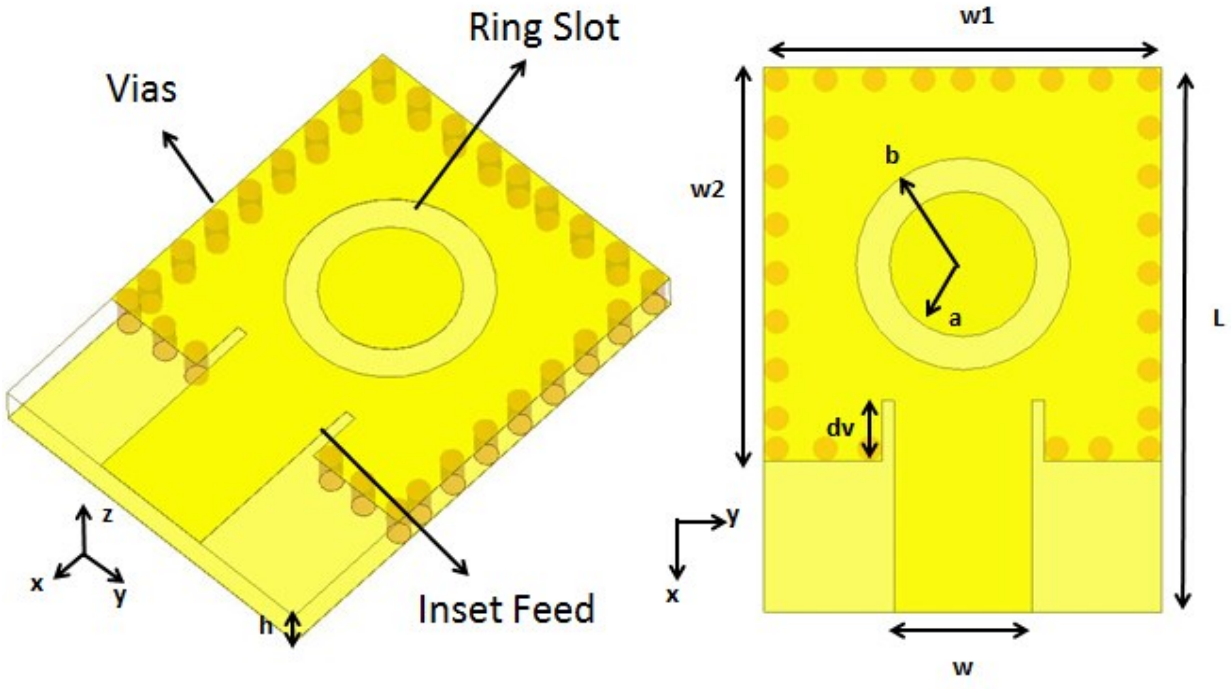

Fig. 20: The SIW ring slot antenna schematic [19].

The S parameters and input impedance of the above SIW ring slot antenna are shown in the following figures.

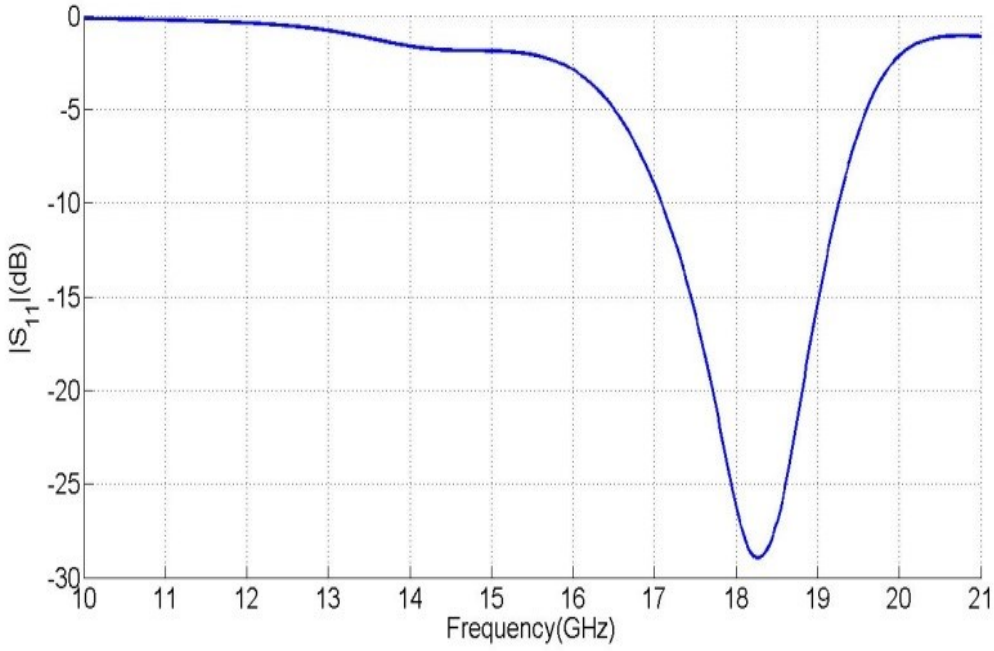

Fig. 21: S parameter for the SIW ring slot antenna.

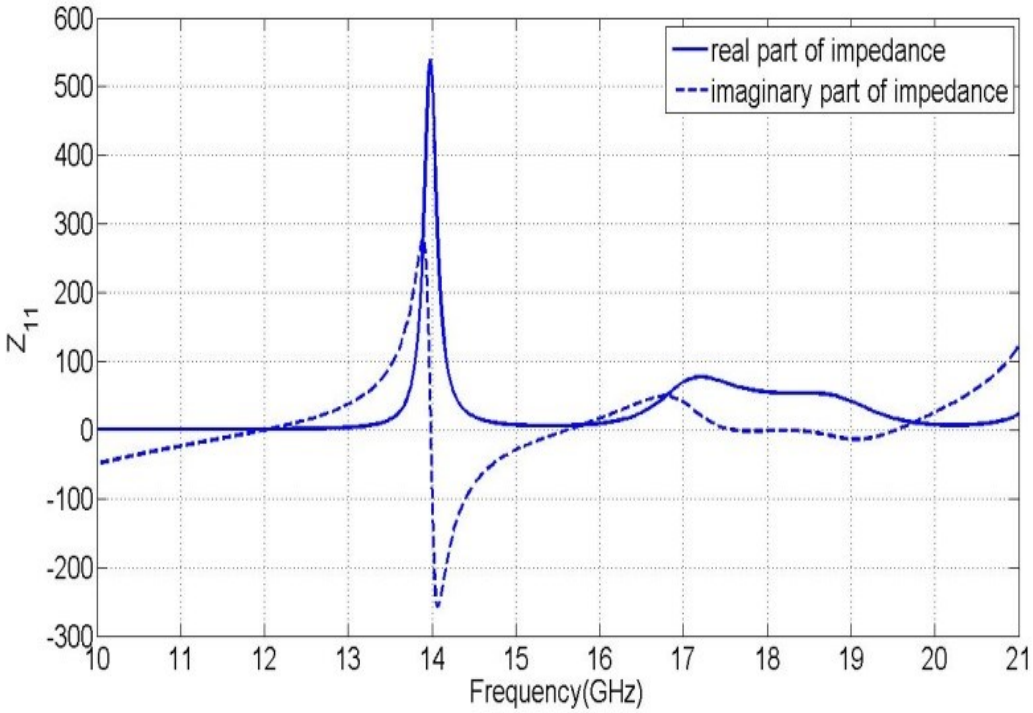

Fig. 22: Input impedance for the SIW ring slot antenna.

When TM110 mode is excited at around 14 GHz, the antenna behaves as a vertical dipole [18]. Moreover, from the input impedance, we find that the cavity acts as a parallel resonator, which produces very high input impedance. Therefore, when 50-ohm transmission line is used as the feed, antenna is poorly matched. The reason we want to mismatch it is that at this mode the antenna shows similar radiation as electric dipole, which is not broadside and limits the energy usage under certain circumstances. Therefore, we are more interested in making use of TM210 mode.

On the other hand, for the TM210 mode at 18 GHz, we can get 12% bandwidth. Also, a flat impedance curve of around 50 ohm is observed at the corresponding frequencies. The working mechanism of the broadband property will be discussed in detail in the following sections. As for the radiation, the antenna will now have a patch-like pattern. The two equivalent magnetic monopoles form an array creating the strongest radiation to the broadside. A 6.8 dB gain is created in simulation, which is shown in Fig. 23.

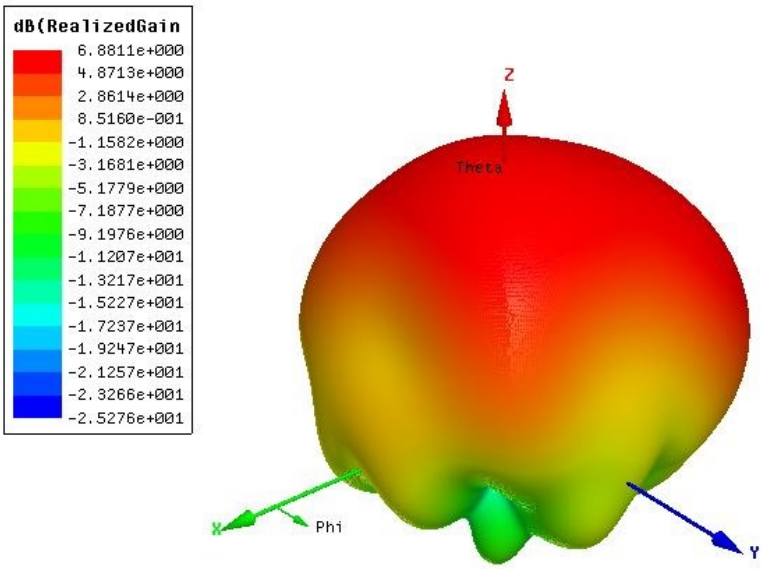

Fig. 23: Realized gain of the SIW ring slot antenna at 18.3 GHz.

Broadband Property & Working Mechanism

The field distribution inside the cavity can help us to understand broadband characteristics of the antenna. Fig. 24 shows the cavity field distribution at 17 GHz, which is the lowest frequency of the band. On the contrary, Fig. 25 shows the field distribution at 19.3 GHz, which is the highest boundary of the working band. In Fig. 24 we also mark the equivalent magnetic current to explain how the antenna works.

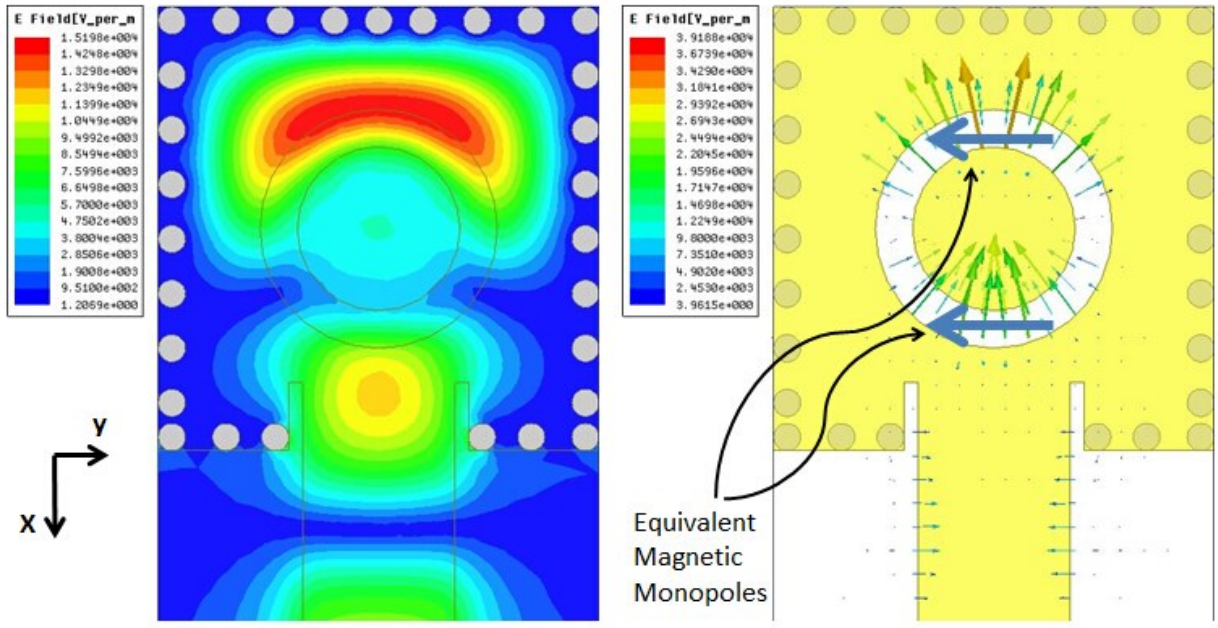

Fig. 24: Working mechanism analysis for the SIW ring slot antenna at the lower working frequency: 17 GHz. Left: internal field pattern. Right: tangential electric field on the slot aperture.

At lowest frequency, we find that the TM210 mode has a very similar field distribution as the cavity mode near the shorting wall. A peak appears between the shorting boundary and the slot. However, below the slot, the field becomes much smaller due to the boundary condition. Therefore, this field distribution creates a strong gradient near the outer edge of the slot, forming an effective radiation in return. Meanwhile it is the outer radius of the ring which corresponds to

the lowest frequency of operation. This explains why it identifies the lowest boundary of the working band. The other peak is shifted toward the feed since the cavity's closure is damaged by the feed when a wide 50 ohm transmission line is used. Finally, the two equivalent magnetic monopoles are created in the direction orthogonal to the feed, creating strongest radiation in the broadside.

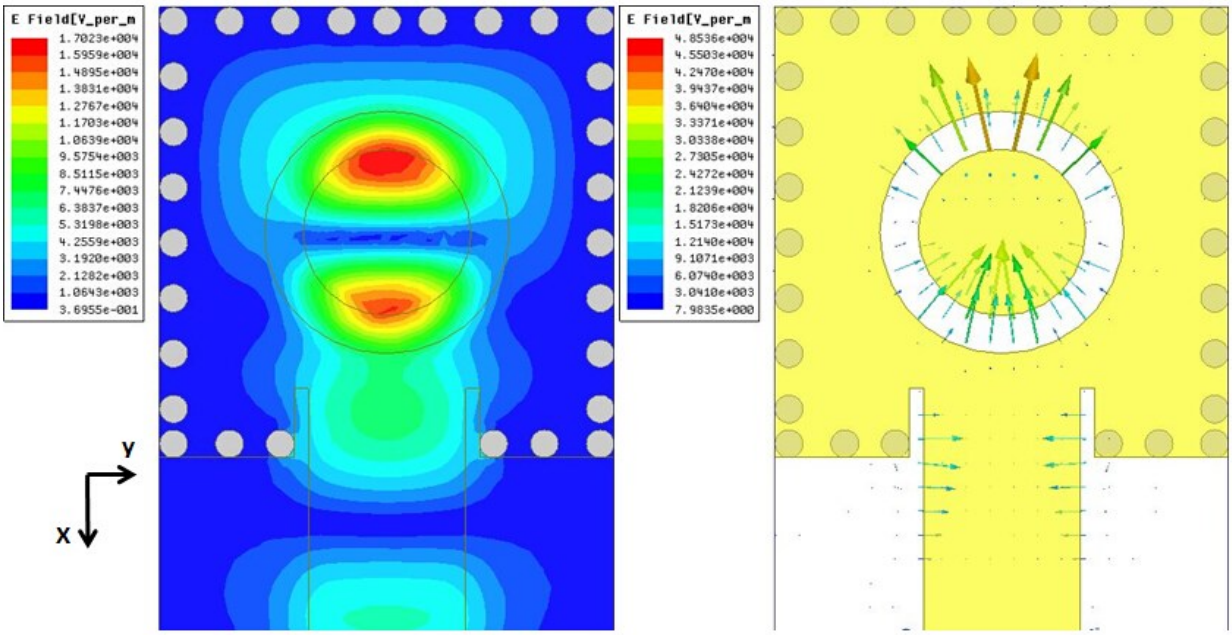

Fig. 25: Working mechanism analysis for the SIW ring slot antenna at the higher working frequency: 19.3 GHz. Left: internal field pattern. Right: tangential electric field on the slot aperture.

At highest frequency of the working band, we find exactly the opposite phenomenon: TM210 mode now shows a shifted cavity behavior that is confined by the open slot. At the location beneath the slot, the field is still small due to boundary conditions. However, the field peaks now shift inside the slot and near the center of the cavity, which can be seen clearly in Fig. 25. Therefore, strong radiation from large electric field gradient is still created, but using the inner ring radius this time. Such a mode determines the highest boundary of the working band. The

working mechanism of this case is very similar to the above one, and both of them help to lower the Q of the cavity and facilitate the matching at the feed. The equivalent magnetic currents are in the same direction, creating maximum radiation in z direction just as the above case.

From above explanations, it is reasonable to believe that at the frequency between the two boundaries, the peak of the electric field will be close to the slot center. Therefore, a smaller gradient will lead to less radiation and worse matching. However, if we plot the field distribution at the central frequency as Fig. 26, which is at around 18.3 GHz, we cannot see the difference clearly. The s parameter in Fig. 21 also does not show any poor matching near the center of the pass band.

However, this phenomenon is indeed happening. But due to the perturbation, it is very difficult to exactly align both peaks right on the aperture, so its effect on the return loss cannot be seen. To understand the mechanism mentioned above, a perturbation of adding central ground pins is proposed.

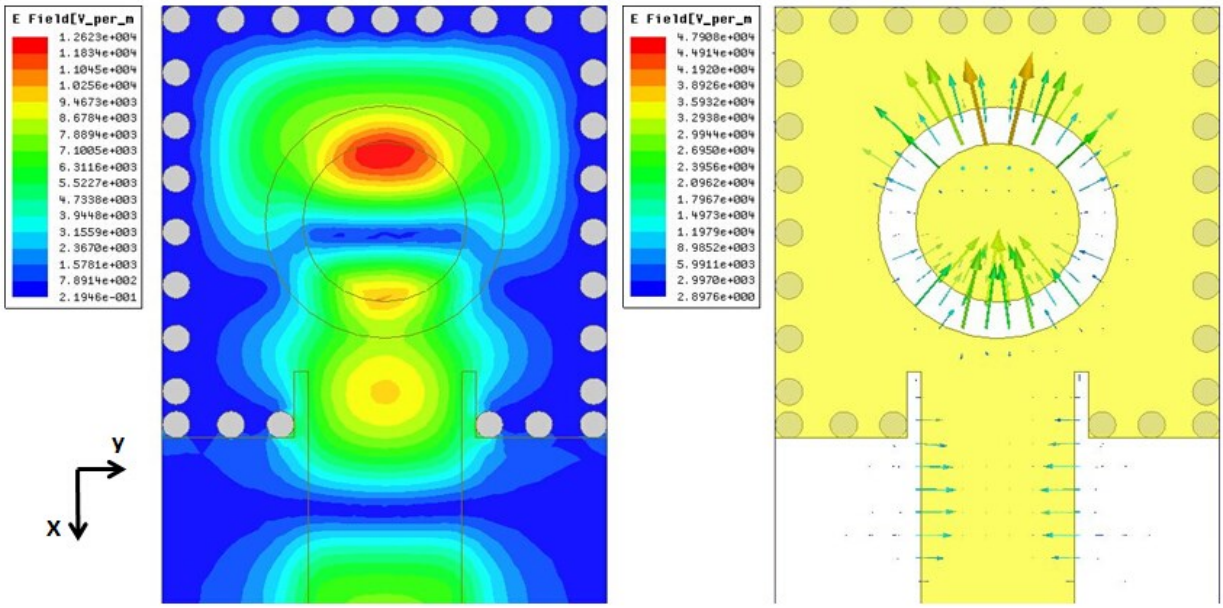

Fig. 26: Working mechanism analysis for the SIW ring slot antenna at the center frequency: 18.3GHz. Left: internal field pattern. Right: tangential electric field on the slot aperture.

Adding extra pins could help to ground fields at certain positions inside the cavity. It was introduced in order to suppress certain modes but actually just adds certain inductive load into the cavity. It has strong perturbation to the field but does not impact the radiation and impedance matching too much in this prototype. We added a through via right at the center of the circular patch as shown in Fig. 27, and got result like Fig. 28. The two cases show similar performance and the case with via clearly demonstrate the two extreme working statuses based on the previous discussion. Moreover, the measured results in the next section also show similar performance, which helps to prove our explanation for the mechanism to some extent.

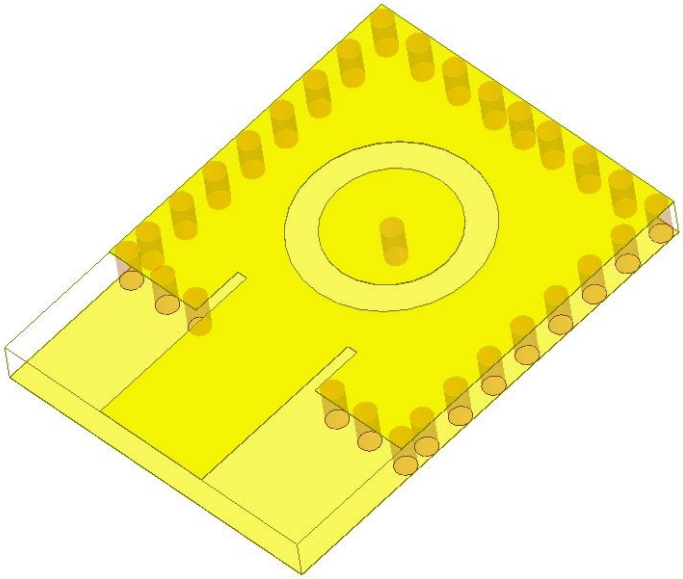

Fig. 27: The schematic of antenna with central ground pin.

The above argument explains why the ring slot antenna is such a good radiator over a wide bandwidth. The ring perturbs the cavity TM210 mode, and since both inner boundary and outer boundary can be used, the antenna can maintain a good radiator during the transition between these two working statuses. Hence the Q of the cavity is low in this case, and a broadband impedance matching for TM210 mode is achieved.

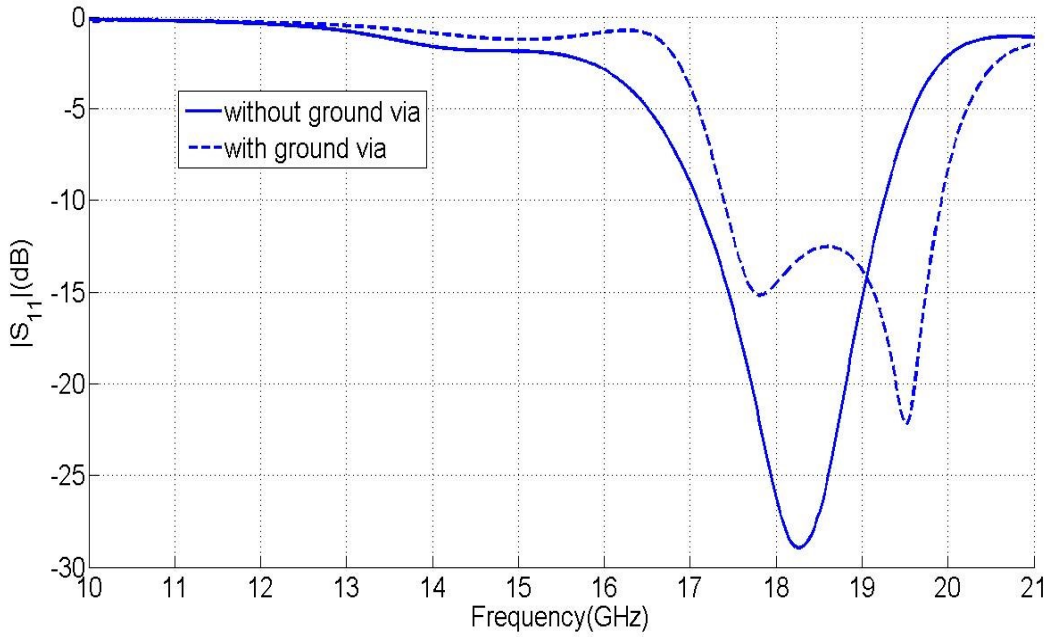

Fig. 28: The S11 of the ring slot antenna with and without a ground via connecting the central circular patch.

Measurement

The above results are based on simulation. After that, a revised structure is built to test its credibility. The structure is based on the prototype shown in Fig. 20. Table 2 also summarizes the physical dimensions. Fig. 29 is a photo of the benchmarked antenna.

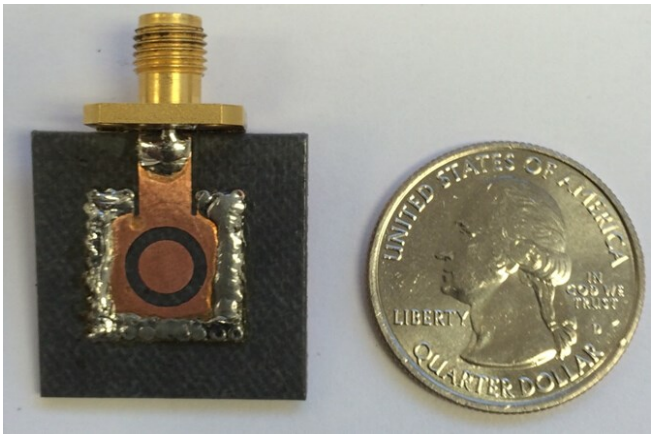

Fig. 29: The benchmarked SIW ring slot antenna.

Table 2: The physical dimensions of the antenna

Parameter	Value	Parameter	Value
W1	13mm	W2	13mm
W	4.5mm	L	18mm
a	2.4mm	b	3.5mm
dv	2mm	h	1.57mm

The measured return loss along with the simulated results is given in Fig. 30. It demonstrates a broad bandwidth from 17.25 GHz to 19.6 GHz. The realized bandwidth is therefore 12.7%. The in-band matching is good, resulting in a 7 dB realized gain at the central frequency 18.25 GHz, as shown in Fig. 31.

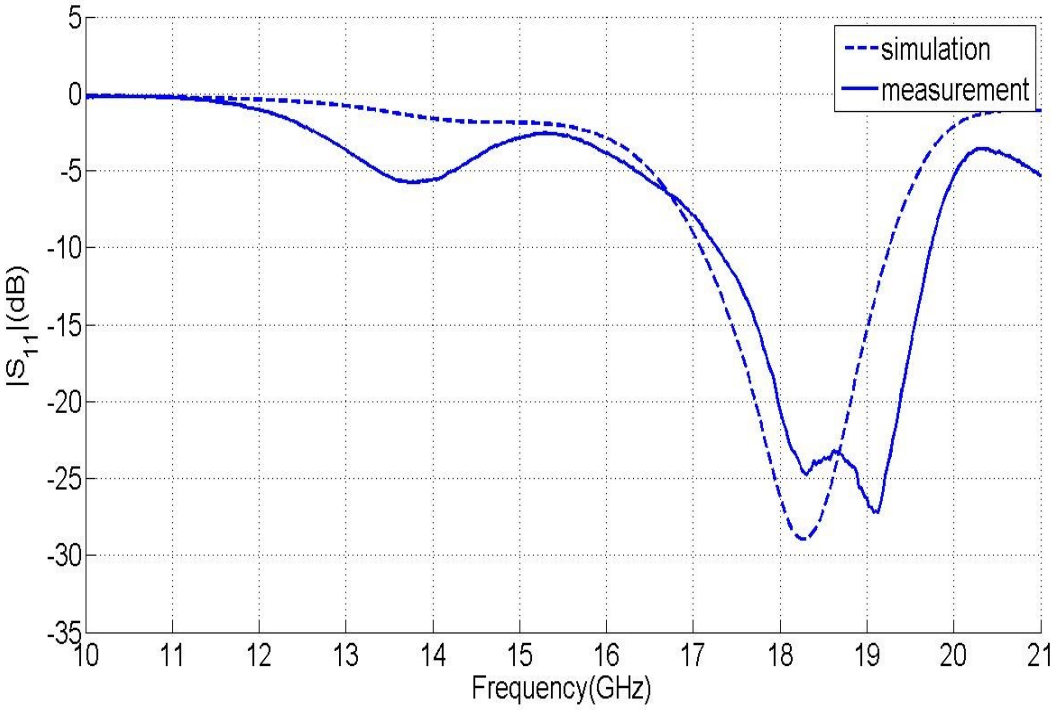

Fig. 30: The S11 of the SIW ring slot antenna.

A 5dB return loss is observed at around 13.8GHz, which corresponds to TM110 mode that should be mismatched. In the simulation the mismatch is satisfactory, but during the implementation, fabrication errors cause the unwanted radiation.

In Fig. 31 a tilted angle of the pattern appears resulting from the alignment issues during the measurement. The antenna was put into a far field chamber in order to measure its radiation pattern. It is hard to align the 0 degree for the co-polarization plane in this case. The power of synthesized sweeper and SNR of spectrum analysizer limit the low-level side lobe to appear clearly in the final result.

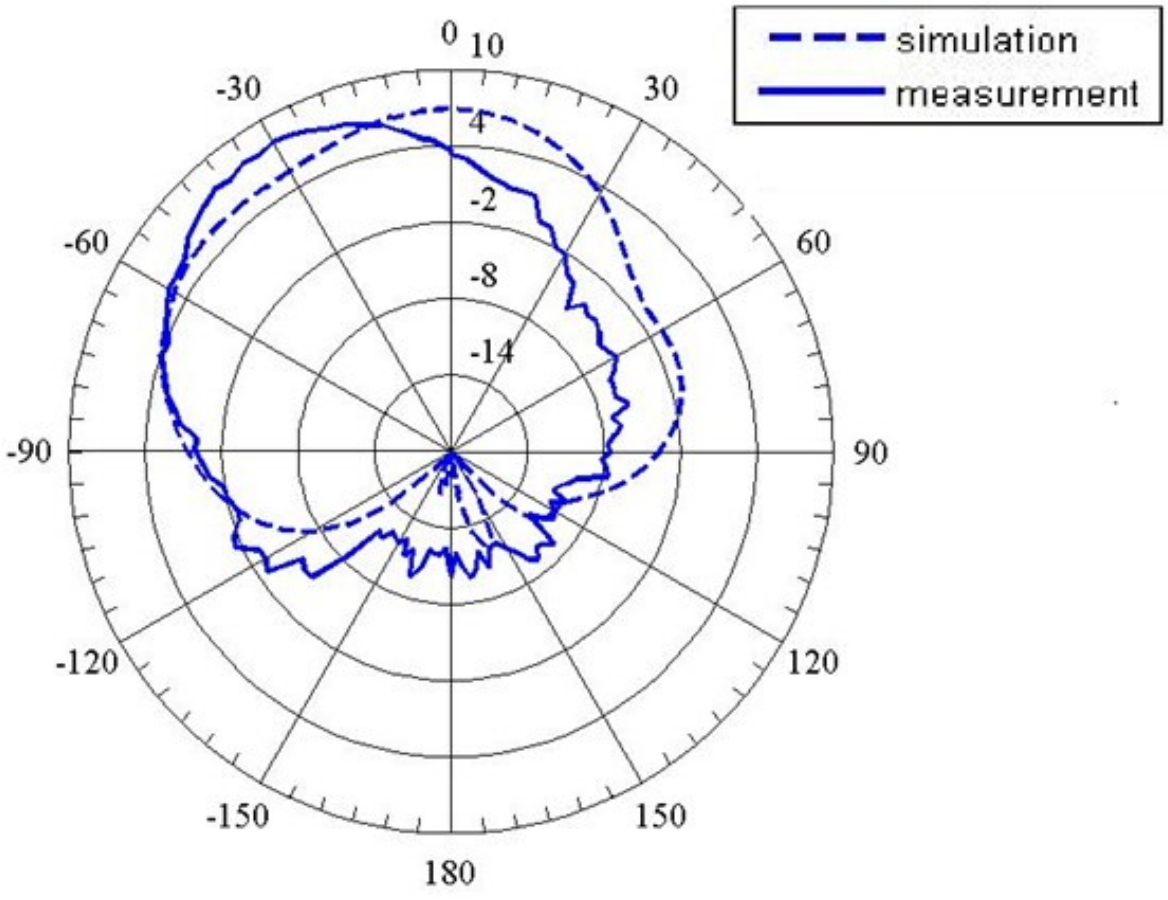

Fig. 31: The co-polarization gain of the SIW ring slot antenna.

Conclusion

In the above section, a broadband design of SIW cavity backed ring slot antenna is proposed and analyzed. The working mechanism is discussed in detail to explain the potential reasons for the broadband characteristics. More than 12% bandwidth and 7 dB realized gain is achieved for broadside radiation. It indicates many potential applications to accommodate the needs of today's communication systems.

REFERENCES

[1] Wu, Ke. "Substrate integrated circuits (SICs) for low-cost high-density integration of millimeter-wave wireless systems." Radio and Wireless Symposium, 2008 IEEE. IEEE, 2008.

[2] Bozzi, Maurizio. "Substrate integrated waveguide (SIW): An emerging technology for wireless systems." Microwave Conference Proceedings (APMC), 2012 Asia-Pacific. IEEE, 2012.

[3] M. Bozzi, A. Georgiadis, and K. Wu, "Review of Substrate Integrated Waveguide (SIW) Circuits and Antennas", IET Microwave Antennas and Propagation, Vol. 5, No.8, pp. 909–920, June 2011.

[4] M. Bozzi, L. Perregrini, and K. Wu, "Modeling of Conductor, Dielectric and Radiation Losses in Substrate Integrated Waveguide by the Boundary Integral-Resonant Mode Expansion Method," IEEE Transactions on Microwave Theory and Techniques, Vol. 56, No. 12, pp. 3153–3161, Dec. 2008.

[5] Chen, Xiao-Ping, and Ke Wu. "Substrate Integrated Waveguide Filter: Basic Design Rules and Fundamental Structure Features." Microwave Magazine, IEEE 15.5 (2014): 108-116.

[6] Chen, Xiao-Ping, Ke Wu, and Zhao-Long Li. "Dual-band and triple-band substrate integrated waveguide filters with Chebyshev and quasi-elliptic responses." Microwave Theory and Techniques, IEEE Transactions on 55.12 (2007): 2569-2578.

[7] Almalkawi, Mohammad, et al. "Design of a dual-band dual-mode substrate integrated waveguide filter with symmetric transmission zeros." Applied Electromagnetics Conference (AEMC), 2011 IEEE. IEEE, 2011.

[8] Shen, Wei, Wen-Yan Yin, and Xiao-Wei Sun. "Miniaturized dual-band substrate integrated waveguide filter with controllable bandwidths." Microwave and Wireless Components Letters, IEEE 21.8 (2011): 418-420.

[9] Rezaee, Mandana, and Amir Reza Attari. "A novel dual mode dual band SIW filter." European Microwave Conference (EuMC), 2014 44th. IEEE, 2014.

[10] StratEdge. *FP118118-1* [Online]. http://www.stratedge.com/pdf/FP118118-1.pdf

[11] Hong, Jia-Shen G., and Michael J. Lancaster. Microstrip filters for RF/microwave applications. Vol. 167. John Wiley & Sons, 2004.

[12] Balanis, Constantine A. Advanced engineering electromagnetics. Vol. 111. John Wiley & Sons, 2012.

[13] Rogers Corporation. TMM Thermoset Microwave Materials [Online]. Available: https://www.rogerscorp.com/documents/728/acm/TMM-Thermoset-laminate-data-sheet-TMM3-TMM4-TMM6-TMM10-TMM10i.aspx

[14] Serrano, Ariana Lacorte Caniato, et al. "Synthesis methodology applied to a tunable patch filter with independent frequency and bandwidth control." Microwave Theory and Techniques, IEEE Transactions on 60.3 (2012): 484-493.

[15] D. Deslandes and K. Wu. "Integrated Microstrip and Rectangular Waveguide in Planar Form", IEEE Microwave and Wireless Component Lett., Vol. II, pp. 68-70. Feb. 2001.

[16]F. Xu and K. Wu, “Guided-Wave and Leakage Characteristics of Substrate Integrated Waveguide,” IEEE Trans. on Microwave Theory and Techniques, Vol. MTT-53, No. 1, pp. 66-73, Jan. 2005.

[17] K. Gong, Z.N. Chen, X.M. Qing, P. Chen, and W. Hong, “Substrate integrated waveguide cavit-backed wide slotantenna for 60-GHz Bands,” IEEE Antennas and Wireless Propagation Letters, vol. 60, no. 12, Dec. 2012.

[18] Chung-Tse Michael Wu and Tatsuo Itoh, “An X-band Dual-mode Antenna using Substrate Integrated Waveguide Cavity for Simultaneous Satellite and Terrestrial Links,” Asia-Pacific Microwave Conference, Nov. 2014.

[19] Chung-Tse Michael Wu, Jun Choi, Hanseung Lee, and Tatsuo Itoh, “Magnetic-Current-Loop Induced Electric Dipole Antenna Based on Substrate Integrated Waveguide Cavity”, IEEE Antennas and Wireless Propagation Letters, pp.519-522, March 2014.